ACS APPLIED MATERIALS & INTERFACES

Research Article

www.acsami.org

3D-Stacked Carbon Composites Employing Networked Electrical Intra-Pathways for Direct-Printable, Extremely Stretchable Conductors

Changju Chae, Yeong-Hui Seo, Yejin Jo, Ki Woong Kim, Wooseok Song, Ki-Seok An, Sungho Choi, Youngmin Choi, Sun Sook Lee,* and Sunho Jeong*

Division of Advanced Materials, Korea Research Institute of Chemical Technology (KRICT), Daejeon 305-600, Republic of Korea

Supporting Information

ABSTRACT: The newly designed materials for stretchable conductors meeting the demands for both electrical and mechanical stability upon morphological elongation have recently been of paramount interest in the applications of stretchable, wearable electronics. To date, carbon nanotube-elastomeric polymer mixtures have been mainly developed; however, the method of preparing such CNT−polymer mixtures as stretchable conductors has been limited to an ionic liquid-mediated approach. In this study, we suggest a simple wet-chemical method for producing newly designed, three-dimensionally stacked carbon composite materials that facilitate the stable morphological elongation up to a strain of 300% with normalized conductivity variation of only 0.34 under a strain of 300%. Through a comparative study with other control samples, it is demonstrated that the intraconnected electrical pathways in hierarchically structured composite materials enable the generation of highly stretchable conductors. Their direct patternability is also evaluated by printing on demand using a programmable disperser without the use of prepatterned masks.

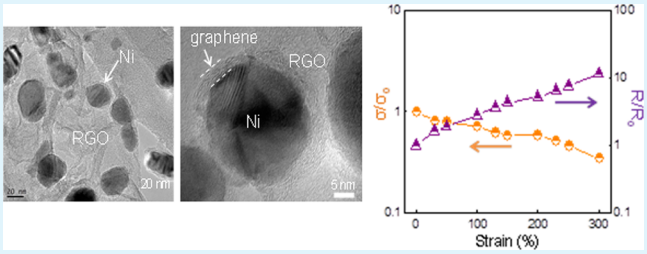

KEYWORDS: *3D, composite, printable, stretchable, conductor*

1. INTRODUCTION

Recently, direct-printable, stretchable conductive materials have drawn tremendous attention in the field of newly emerging stretchable electronics,[1−3] as stretchable interconnectors are essential building blocks in integrating wearable active devices,[4] and a variety of electrical signal-based strain/pressure sensor devices could be exploited from them.[5] At an early stage of development, carbon nanotube (CNT)−polymer mixtures were widely researched owing to the characteristic low volumetric threshold for percolation conduction of one-dimensional carbon materials.[1−3,6−10] Then, it has been demonstrated that high electrical conductivity over the limit of carbon-based mixtures is attainable by incorporating highly conductive metallic fillers into the composites of CNT and polymeric substances.[11−14]

However, to date, the use of CNT−polymer mixtures into which metallic conductive fillers can be inserted has been limited to the case of blending ionic liquid-treated CNTs and elastomeric polymers.[6−10] To attain high electrical conductivity in stretchable CNT−polymer mixtures, a sufficient amount of CNTs, enough to allow for percolation conduction, should be incorporated with a morphological homogeneity in elastomeric polymers; however, it is highly demanding to disperse uniformly the bundle-like CNT assemblies inside elastomeric polymers. To address this issue, combination approaches of physical and/or chemical mixing have been demonstrated. Through a high-shear extruding process[15] or high-pressure jet-milling along with the chemical role of ionic liquids in forming swollen bucky CNT-gels,[8] CNTs were successfully incorporated with a solid loading even up to 15 wt %. With the introduction of a perforated morphological structure[7] or acidic post-treatments,[9] both conductivity and stretchability were further improved. However, as claimed in reports suggesting, for the first time, this ionic liquid-based methodology,[7,8] there are critical criteria in the preparation of ionic liquid-based CNT/elastomer mixtures: (1) a proper mixing ratio of ionic liquid and CNTs, (2) chemical compatibility between ionic liquid and elastomeric polymer, (3) the use of extremely high aspect ratio CNTs, and (4) the sophisticatedly controlled mixing process for dispersing CNTs without morphological degradation. Alternatively, a conceptual study of three-dimensional (3D) carbon web-like structures was suggested using CNT forests chemical vapor deposition (CVD)-grown on Si wafers, demonstrating the paramount importance of hierarchical morphology in designing conductive materials with extreme stretchability.[16] However, even with the potential of hierarchically structured materials as high-performance stretchable conductive ones, 3D-stacked carbon materials, so far, have

Received: November 19, 2014
Accepted: February 3, 2015
Published: February 3, 2015

DOI: 10.1021/am5080634
ACS Appl. Mater. Interfaces 2015, 7, 4109−4117

not been exploited in the form of direct-printable wet-phase through easily scalable chemical pathways,[17−19] other than vacuum-based processes on rigid silicon substrates, due to the lack of a synthetic strategy.

In this study, we demonstrate, for the first time, a wet-chemical method to forming three-dimensionally stacked carbon composites using graphene oxides (GOs) and Ni nanoparticles as starting materials. Multilayer graphenes are grown on the surface of Ni nanoparticles welding individual thermally reduced GO sheets, allowing for fully interconnected carbon sheets with internal electrical pathways. Through the incorporation of a polystyrene−polyisoprene-polystyrene (SIS) triblock copolymer as an elastomer and multiwall carbon nanotubes (MWCNTs) as a bridging conducting moiety, direct-printable composite pastes are prepared, enabling the facile formation of stretchable conductors exhibiting normalized conductivity variation of only 0.34 even under elongation of 300%.

2. EXPERIMENTAL METHODS

2.1. Synthesis of Ni Nanoparticles. Ni(II) acetylacetonate ($Ni(C_5H_7O_2)_2$, 95%), oleylamine ($C_{18}H_{37}N$, 70%), oleic acid ($C_{18}H_{34}O_2$, 90%), phenylhydrazine ($C_6H_5NHNH_2$, 97%), and toluene ($C_6H_5CH_3$, anhydrous, 99.8%) were purchased from Aldrich, and used as received without further purification. Ni nanoparticles were synthesized via the chemical reduction of Ni ions in oleylamine under an inert atmosphere. 5.0 g of Ni acetylacetonate and 4.2 g of oleic acid were added into a three-neck round-bottomed flask containing 71.8 g of oleylamine. The flask was fitted with a reflux condenser and a mechanical stirrer, and the solution was purged with Ar for 60 min. Then, 20 g of hydrazine was injected at 90 °C with an injection rate of 2 mL/min. The solution was heated to 240 °C, and the reaction was continued for 60 min. After completion of the synthesis reaction, the synthesized Ni nanoparticles were separated by centrifugation in air and washed using toluene and chloroform with an equivalent volume ratio. After dispersion in the excessive amount of toluene, the synthesized Ni nanoparticles were kept in air without additional surface-passivation procedures.

2.2. Synthesis of (Reduced) Graphene Oxide. GOs were prepared by the subsequent reaction of oxidation/exfoliation for natural graphite flakes (Sigma-Aldrich), in a manner modified from Hummers method. A mixture of natural graphite flake (5.0 g) and $NaNO_3$ (3.75 g) was placed in a 2 L round-bottom flask containing 375 mL of H_2SO_4 (95%) with stirring in an ice bath. Next, 22.5 g of $KMnO_4$ was added slowly, while the reaction temperature was kept below 20 °C. Then, the flask was placed in an oil bath at 30 °C and removed from the oil bath 2 days later. After the solution cooled in air, 700 mL of 5 wt % H_2SO_4 was slowly added to the flask, and stirring was continued for 2 h. Next, 15 mL of 30 wt % H_2O_2 was slowly added with the color change of the suspension from dark brown to yellow, and stirring was continued for 2 h. The as-obtained graphite oxide was purified with distilled water several times by centrifugation. GO sheets were exfoliated from graphite oxide by ultrasonication. The products were redispersed in distilled water. The dispersed GOs were used to formulate the pastes. In the case of a control experiment, a GO solution was immersed in liquid nitrogen, and then freeze-dried for 48 h. Chemically reduced GOs (cRGOs) were prepared using hydrazine monohydrate ($H_2N_2{\cdot}H_2O$, 80%, DC Chemical Co.). The GO solution of 1 mg/mL was immersed in a flask containing 0.1 M $H_2N_2{\cdot}H_2O$ and stirred at 80 °C with a reflux for 16 h. Then, the reaction solution was cooled in air, and the cRGOs were purified with distilled water several times by centrifugation. The resulting cRGOs were freeze-dried in the same way as the GOs.

2.3. Preparation of 3D Stacked Carbon Composites (3D-Cs). Ni nanoparticles were collected from the suspension by centrifugation at 24 000 rpm for 15 min using a mixture of toluene and chloroform with an equivalent volume ratio. To obtain the homogeneity in mixing different materials, the wet precipitates not accompanied by a drying process, were used for further experiments. The wet Ni nanoparticle precipitates obtained after complete removal of the supernatant solutions, contain some fraction of solvents; thus, to confirm the preparation of reproducible wet precipitates, the fraction of solvents was measured by weighing both the as-precipitated and fully dried powders for 5 different samples. The solvent fraction was measured to be 7.96 wt %. Then, 0.12 g of the obtained Ni wet precipitates was added to 8 g of DCB. The aqueous GO suspension, with a solid loading of 3 mg/mL, of 80 mL was mixed with 160 mL of methyl alcohol, followed by centrifugation at 24000 rpm for 30 min. Then, the precipitated GOs were redispersed with 240 mL of methyl alcohol and centrifuged again under the same conditions to eliminate the remaining water from the GO precipitates. The fraction of solvent in the GO wet precipitates was also measured to be 95.9 wt %. The yields after a thermal annealing at 400 °C were 94.1 and 38.9 wt % for Ni nanoparticles and GOs, respectively. To prepare Ni-GO composite with an equivalent weight ratio after a thermal annealing at 400 °C, 6.2 g of the GO wet precipitates was added to the prepared Ni suspension with an additional 7 g of DCB, followed by the first sonication for 3 min, the second sonication for 3 min after adding 15 g of NMP, and the third−fifth sonications, each for 3 min after adding both 10 g of DCB and 10 g of NMP. The completely homogenized GO-Ni nanoparticle suspension was centrifuged at 24000 rpm for 20 min, and the resulting composite materials were dried at 80 °C for 3 days, and then heat-treated at 400 °C under an Ar atmosphere with a flow rate of 100 sccm for 2 h. Graphene was synthesized using a conventional thermal chemical vapor deposition system. The prepared GO-Ni composite powders were loaded in an alumina boat, placed in a reactor, and heated from room temperature to 900 °C with the introduction of H_2 gas (100 sccm) for 30 min. When the reactor was heated to the target temperature, methane (CH_4, 25 sccm) was introduced as a carbon feedstock with H_2 gas under 5 Torr for 30 min to synthesize the graphene. The CH_4 was turned off, and the reactor was cooled to room temperature with flowing H_2 gas.

2.4. Paste Formulation, Film Formation, and Direct Printing. The pastes were formulated using MWCNTs, a mixture of MWCNTs and GOs, a mixture of MWCNTs and cRGOs, or a mixture of MWCNTs and 3D-Cs. The MWCNTs (97%, ∼20 nm in diameter, and ∼10 μm in length) were purchased from Applied Carbon Nano Technology. To break soft agglomerates, MWCNTs were dispersed in DCB with a sonication for 3 min, followed by centrifugation at 24 000 rpm for 20 min. The collected MWCNTs were manually mixed with a preformed SIS triblock copolymer solution in an agate mortar for 5 min. The manually blended paste was finally mixed using a rotation/revolution mixer (ARE-310, THINKY) at 2000 rpm for 5 min with a further deforming process at 2200 rpm for 1 min. To formulate the composite paste, the GOs, cRGOs, or 3D-Cs were manually mixed with identically prepared MWCNTs and SIS triblock copolymer solution in an agate mortar for 5 min, and finally mixed using the rotation and revolution mixer. The compositional details of all pastes are summarized in Table S1 (Supporting Information) with a simple summary of their electrical properties. The resulting pastes were poured into preformed molds and covered with lids, followed by drying at 80 °C for 3 h. For preparation of the molds, a mixture of polydimethylsiloxane (PDMS) precursor and curing agent (Sylgard 184, Dow Corning Corp.) with a ratio of 10:1 (w/w) was manually blended for 10 min. This was poured into a Petri dish with a 125 μm thick-polyethylene terephthalate (PET) film, and after degassing for 1 h at room temperature, the molds were hardened at 60 °C overnight. The lids were made by the same method without PET films. Arbitrary patterns were produced by printing the resulting composite paste on an elastomeric substrate through a 350 μm nozzle using a programmable dispenser (SHOT mini 200S, Musashi Engineering) with a moving speed of 20 mm/s. Then, the printed patterns were dried at 80 °C for 30 min.

2.5. Characterization. The size and shape of the synthesized Ni nanoparticles were observed by scanning electron microscopy (SEM, JSM-6700, JEOL). The crystal structure of Ni nanoparticles was analyzed by X-ray diffractometry (XRD, D/MAX-2200 V, Rigaku) and

DOI: 10.1021/am5080634
ACS Appl. Mater. Interfaces 2015, 7, 4109−4117

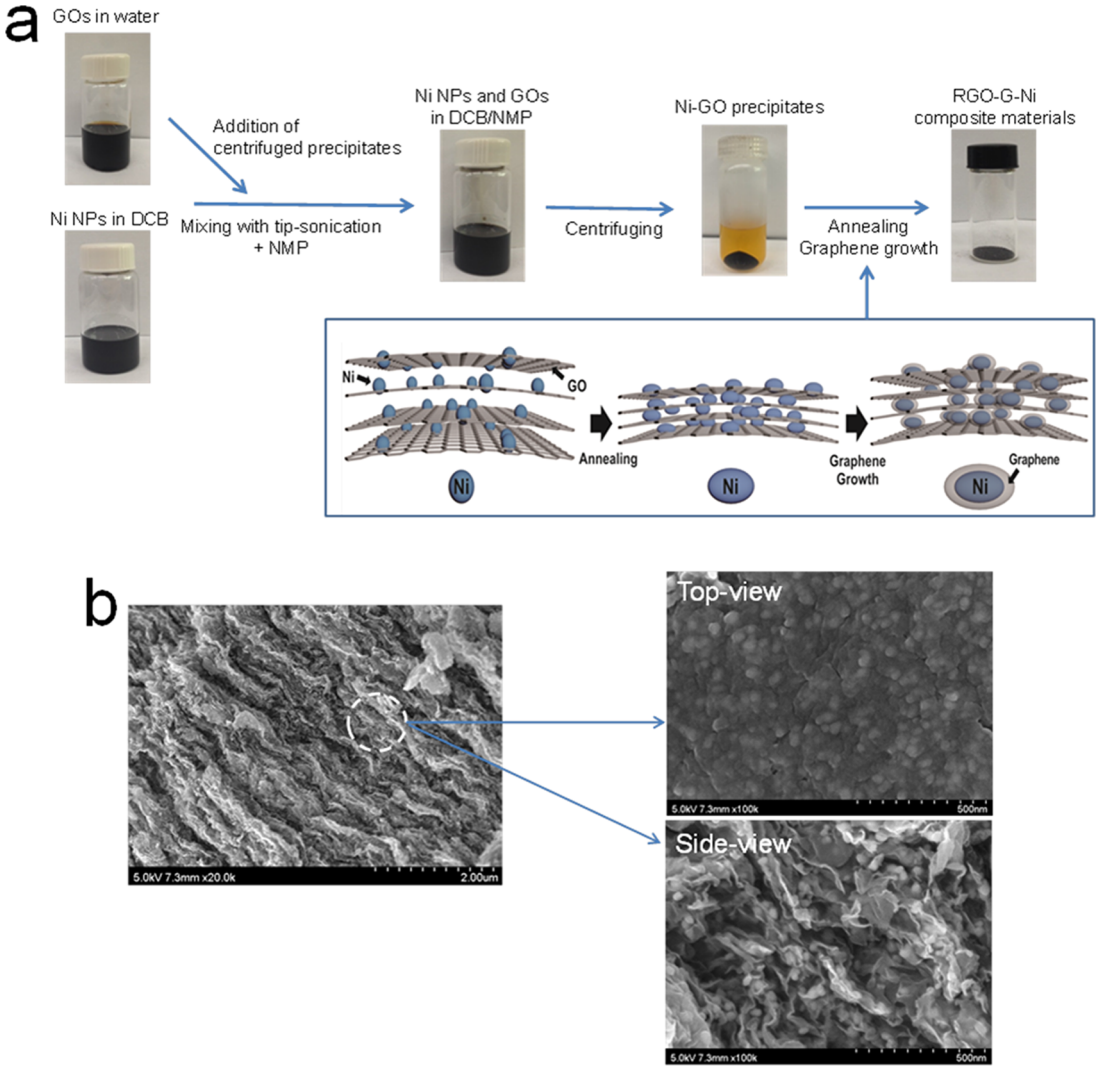

Figure 1. (a) Schematic diagram showing the sequential procedure of preparing 3D-Cs; (inset) schematic of thermally driven welding by nanosized Ni particles during annealing at 400 °C and the formation of hierarchically structured composites by the formation of multilayer graphene along the surface of Ni nanoparticles during the CVD-graphene growth process. (b) SEM image of resulting 3D-Cs.

the chemical structural analysis of Ni nanoparticles was performed by X-ray photoelectron spectroscopy (XPS, K-Alpha, Thermo Fisher Scientific). The morphology and Raman spectra of 3D-Cs were observed by high-resolution transmission electron microscopy (TEM, Tecnai G2 20, 200 kV) and micro Raman spectroscopy (Renishaw, 514 nm, Ar^+ ion laser), respectively. The TEM samples were prepared by drop-casting on lacey carbon TEM grids. The resistance was analyzed by an ohm-meter (2316-V0001, Burster) with a bending/stretching machine (PMC-1HS, Autonics). When the film with a specific volume is stretched under a given strain, the volume of total film is not varied and the length of specimen is elongated. The length in a stretched specimen can be easily recorded, from which the cross-sectional area was calculated. The conductivity of stretched film was obtained based on the dimension, length and cross-sectional area of the sample, and the measured resistance.

3. RESULTS AND DISCUSSION

Figure 1a shows the sequential procedure of preparing the 3D-stacked carbon composites. First, we synthesized nickel nanoparticles using a solvothermal synthetic method, in which Ni acetylacetonate, oleylamine, oleic acid, and phenylhydrazine were used as a nickel precursor, a solvent, a capping molecule, and a reducing agent, respectively. After a vigorous reaction at 240 °C, the synthesized nanoparticles were extracted and washed by centrifugation with toluene. The resulting nickel nanoparticles were readily dispersed in dichlorobenzene (DCB) without further surface capping procedures. As seen in the SEM, high-resolution TEM, XRD, and XPS results (Figures S1−S4, Supporting Information), spherical Ni nanoparticles with a diameter of ∼30 nm were synthesized, and the thickness of surface shell layer was measured to be ∼2.5 nm. The surface layer was composed of both surface oxide and organic capping molecules.[20] The GOs were prepared using a modified Hummers method. To intercalate individual GO sheets with 30 nm sized Ni nanoparticles, the Ni nanoparticle suspension in DCB and the GOs were homogeneously mixed by a simple sonication method in the presence of excessive *N*-methyl-2-pyrrolidone (NMP) as a cosolvent. Note that Ni nanoparticles tend to be easily oxidized during synthetic reactions at elevated temperatures for reducing nickel ions, resulting in the preferential formation of nickel oxide phase. To prevent chemical oxidation, organic solvents are more favorable as a reaction medium over H_2O; therefore, surface capping molecules for both suppressing the interparticular agglomeration and stabilizing the surface Ni

DOI: 10.1021/am5080634
ACS Appl. Mater. Interfaces 2015, 7, 4109−4117

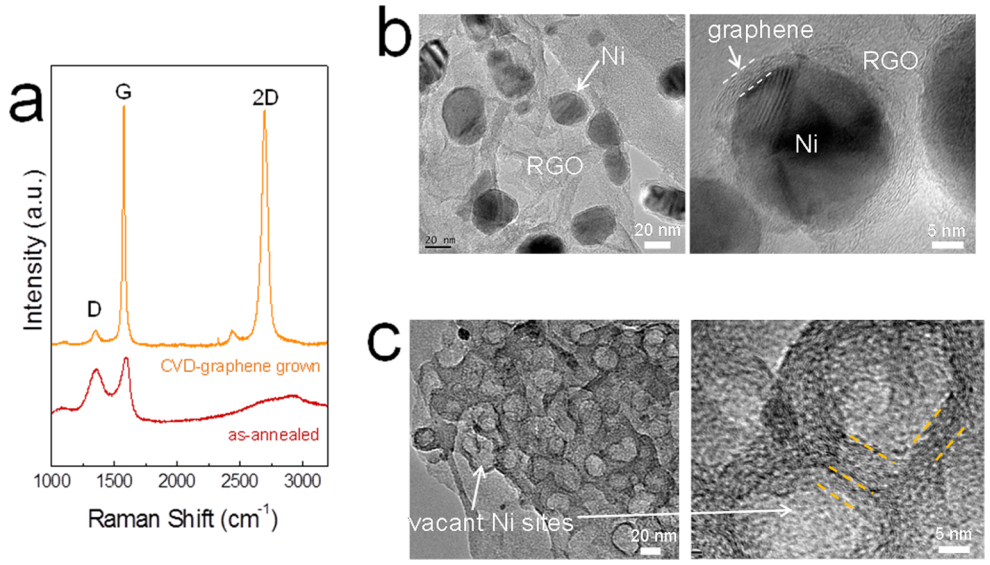

Figure 2. (a) Raman spectra for as-annealed and CVD-graphene grown composite materials. HRTEM images for (b) CVD-graphene grown composite materials and (c) corresponding composite materials after chemical etching of Ni phase.

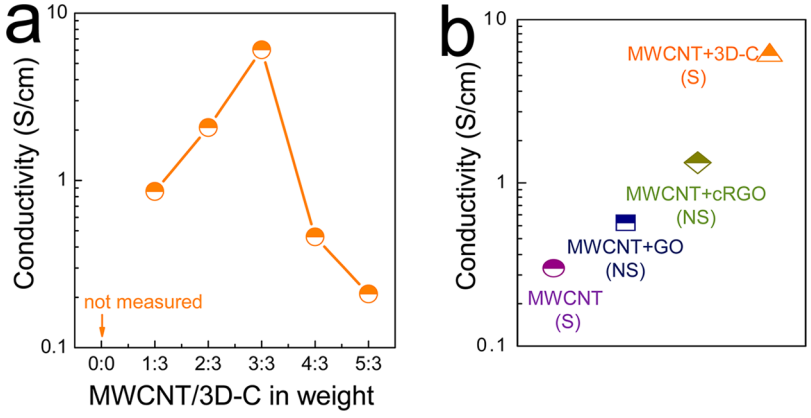

Figure 3. (a) The conductivity variation of MWCNT/3D-C stretchable conductors depending on the weight ratio of MWCNT to 3D-C. The conductivities were measured in an unstrained state. (b) Comparison of conductivity and stretchability for various composite electrodes prepared using MWCNT, a mixture of MWCNT and GO, a mixture of MWCNT and cRGO, and a mixture of MWCNT and 3D-C. For MWCNT/GO, MWCNT/cRGO, and MWCNT/3D-C composite electrodes, the weight ratio of MWCNT to GO, cRGO, or 3D-C was 3:3. Stretchability is indicated as (S) stretchable or (NS) non-stretchable.

atoms are chosen to be compatible to the corresponding organic solvents. GOs are dispersed in polar solvents, for example, H_2O, due to their intrinsic surface chemical structure. Thus, the development of a wet-chemical methodology for mixing GOs and Ni nanoparticles with distinctively different surface properties is quite difficult; to resolve this issue, in this study, NMP-assisted sono-chemical hybridization is proposed without the involvement of other complicated procedures. It was clearly observed that Ni nanoparticles were distributed uniformly without the formation of agglomerates, expanding the interplanar displacement between neighboring GO sheets (Figure 1b).

Then, the GO-Ni composites were subjected to thermal annealing at 400 °C under an inert atmosphere, as the Ni nanoparticle acts as a thermally driven welding agent. For the case of metal particles, morphological deformation as a semi-wet phase is triggered by thermal annealing at temperatures close to their melting point.[21−23] The melting point of bulk Ni phase is 1428 °C, but as the particle size approaches the level of a few tens of nanometers, the melting point starts to decrease drastically due to the energetically unstable nature of surface atoms. In fact, electrically resistive Ni nanoparticle assemblies, formed by drop casting of a Ni nanoparticle suspension on a glass substrate, were transformed into interwelded bulk structures after annealing at 400 °C under an inert atmosphere, showing the resistivity of 230 $\mu\Omega$·cm. The presence of a surface oxide layer adversely affects the interparticular mass transport and, in turn, the electrical conductivity, as proven previously in CuO/Cu core/shell nanoparticles.[24] The slightly higher resistivity than that of bulk Ni phase, 6.8 $\mu\Omega$·cm, indicates the adverse impact of even a thin surface oxide layer. This is further evidence of the importance of synthesizing Ni nanoparticles in organic solvents.

Then, the multilayer graphenes were formed by following CVD-graphene growth process at 900 °C under a constant flow of H_2/CH_4 gas, while the GOs were thermally reduced. As seen in the Raman spectra (Figure 2a), the representative GO fingerprints, a D-band at 1353 cm^{-1} and a G-band at 1593 cm^{-1}, were apparent before the growth process. After the synthesis of graphene, four interesting features were observed:

DOI: 10.1021/am5080634
ACS Appl. Mater. Interfaces 2015, 7, 4109−4117

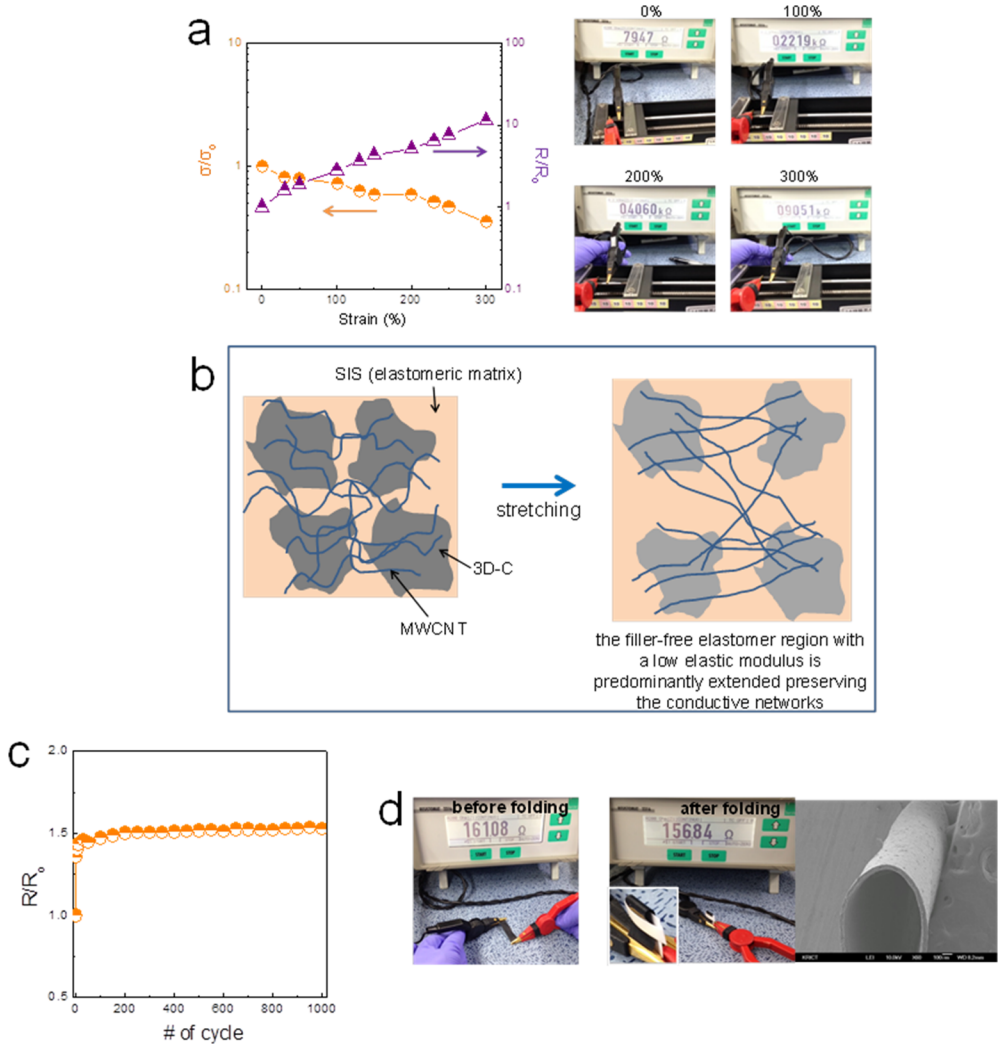

Figure 4. (a) The variation of normalized conductivity and resistance for MWCNT/3D-C composite electrodes as a function of strain up to 300%. The images show the real values of resistance measured for composite electrodes stretched with strains of 0, 100, 200, and 300%. (b) Schematic diagram showing the morphological evolution in composite electrodes under a stretched condition. (c) The variation of normalized resistance for MWCNT/3D-C composite electrodes during a repeated stretching test under a strain of 50%. (d) Photographs showing the real values of resistance measured for MWCNT/3D-C composite electrodes before/after a folding test, and SEM image for folded MWCNT/3D-C composite electrodes. The weight ratio of MWCNT to 3D-C was 3:3.

the appearance of 2D-band at 2696 cm^{-1}, a significant red shift of the G-band from 1593 to 1575 cm^{-1}, the decrease of the full-width at half-maximum (fwhm) of the G-band from 85.1 to 21.0 cm^{-1}, and the significant increase, from 1.2 to 8.9, of intensity ratio (I_G/I_D) of the G-band to the D-band. In addition, the intensity ratio (I_{2D}/I_G) of the 2D band to the G band was measured to be 0.9, indicative of the formation of multilayer graphene. Figure 2b shows the HRTEM images for the synthesized 3D-stacked carbon composites. The Ni nanoparticles were firmly located on reduced graphene oxides (RGOs), and the multilayer graphenes were formed uniformly on the surfaces of the Ni nanoparticles. By the reductive environment at elevated temperatures during the CVD-graphene growth process, the thin surface NiO layer is reduced; thus, it is presumed that the surface layer is attributable to carbon layers. As for the thermogravimetry analysis (TGA) data (Figure S5, Supporting Information), the Ni nanoparticles thermally annealed at 400 °C were almost free of capping molecules. To further clarify the formation of 3D interconnected structures, we etched out the Ni phase using a hydrochloric solution. As shown in Figure 2c, uniform porous structures were obtained without the collapse of the framework skeletons, indicative of the presence of Ni phase in firm contact with RGOs and graphenes. This 3D-stacked carbon composite is referred as 3D-C in this study.

To evaluate the applicability of these materials as stretchable conductors, we formulated pastes comprising SIS and 3D-Cs with DCB as a solvent, and the resulting pastes were poured into preformed molds, followed by drying at 80 °C. In the case of only 3D-C paste, its conductivity was measured to be out of range in ohm-meter with a measuring limit of 200 kΩ. This is due to the lack of bulk conductive pathways between neighboring 3D-Cs; therefore, additional MWCNTs were added as a conductive moiety to macroscopically bridge the 3D-Cs. Details of the composition of each constituent material in the pastes are presented in Table S1 (Supporting Information). As shown in Figure 3a, as expected, with increasing the weight ratio of MWCNTs to 3D-Cs up to 3:3, the conductivity increased proportionally, reaching 6.04 S cm^{-1}. However, with a weight ratio over 4:3, the conductivity

DOI: 10.1021/am5080634
ACS Appl. Mater. Interfaces 2015, 7, 4109−4117

decreased drastically to the value of 0.46 S cm^{-1}. When more 3D-Cs were incorporated, films with uniform surface morphologies were not obtainable owing to extremely thick rheological properties. The conductivity of films prepared from a 3D-C free, MWCNT-based paste was measured to be 0.3 S cm^{-1}. The improvement in conductivity was by a factor of 20.1 when the proper amount of 3D-C was incorporated. This drastic enhancement of the electrical property demonstrates the predominant role of 3D-Cs in enhancing the conductivity inside the elastomeric polymer matrix.

To further elucidate the critical role of 3D-Cs, either GOs or chemically reduced graphene oxides (cRGOs) was incorporated instead of 3D-Cs in formulating pastes as a control experiment. In preparing thermally driven RGOs, the GOs were scattered away in the overall space inside a tube furnace during annealing under an inert atmosphere, unlike the case of 3D-Cs with the interwelding agent, Ni nanoparticles; thus, cRGOs were prepared using a hydrazine-based chemical treatment. As shown in Figure 3b, the conductivity of the 3D-C-based conductor appeared to be higher by factors of 10.6 and 4.7 compared to that of GO- and cRGOs-based conductors, respectively. In these experiments, the compositional ratios of MWCNT/GO and MWCNT/cRGO were optimized to obtain the best electrical conductivities (Figures S6 and S7, Supporting Information). The presence of Ni phase in 3D-C based conductor does not contribute significantly to the conductivity. It has been reported that in Ag-CNT−polymer mixtures, in order for triggering a percolation conduction, the metallic phase with the weight ratio of metal to CNT over 40 should be incorporated, preserving the closely contacted interparticular morphology. In this study, the weight ratio of Ni to carbon is less than 1, and the individual Ni nanophases are completely separated by neighboring carbons. The higher conductivity, compared with MWCNT/GO and MWCNT/cRGO-based conductors, indicates the importance of intraconductivity in 3D-stacked carbon materials. In GO-derived carbon materials, the electrical conductivity in a direction perpendicular to a stacked film surface is poor due to the lack of sheet-to-sheet electrical junctions. Also, for MWCNT/GO and MWCNT/cRGO composites, both films were not stretchable due to the structural rigidity of highly stacked carbon materials when prepared with the compositional ratio exhibiting the best conductivities.

Figure 4a shows the variations of normalized conductivity and resistance for 3D-C-based conductors, with a MWCNT/3D-C ratio of 3:3, as a function of uniaxial strain. Notably, as shown in the photograph images, the film structures were preserved well, even under a strain as high as 300%, and the variations of normalized conductivity and resistance were 0.34 and 11.4, respectively, when the films were stretched up to 300%. The 3D-C-based composite electrode exhibited conductivity of 6.0 S cm^{-1} under an unstrained condition, and of 2.1 S cm^{-1} under a strain of 300%. For the application of a carbon-based matrix where highly conductive metallic constituents can be additionally incorporated, high stretchability with moderate electrical conductivity is of paramount importance. A carbon-based percolation framework should be present for a low threshold for metallic constituents, and such carbon-based elastomeric materials should exhibit rubber-like stretchability, as the incorporation of additional metallic fillers, which in general occupy a volume fraction of 20−40% in dried samples,[11−14] inevitably leads to the drastic degradation of elastic properties. To date, in the case of representative ionic liquid-CNT-based printable pastes, the highest conductivity was reported to be 6 S cm^{-1}, when the films were stretched by a strain of less than 134%, at which point they break.[6] The variation of normalized conductivity was 0.10 under a strain of 134%. This indicates that the 3D-C composite materials prepared in this study exhibit superior electrical/mechanical properties as a highly stable stretchable conductor, even though they were wet-chemically derived by the newly developed synthetic scheme. The conductivity of CNTs-ionic liquid-based electrodes can be improved drastically over 18 S cm^{-1} after a nitric acid vapor treatment;[9] however, this unique method cannot be adoptable in certain practical applications in which there are other underlying active layers that are chemically vulnerable against highly acidic fumes. The conductivity of an untreated, pristine electrode was reported to be 0.34 S cm^{-1}. Additionally, in some cases, intentionally incorporated ionic liquid has been removed for improving the electrical conductivity of finally dried films,[10] and the plausible origin for the role of ionic liquid still has not been not explained,[1,2] even with the suggestion of cation-π interaction between the surface of CNTs and the imidazolium ionic liquid, weak van der Waals interactions, or electrostatic interactions.[25]

In previous studies demonstrating 3D-interconnected carbon materials as stretchable conductors, the stretchability of 300% was achievable with an elastomer overlayer, but the conductivity was limited to 0.2−1 S cm^{-1}.[16] Also, conductors stretchable by more than 200%, to date, have been demonstrated with predeformed substrates, on the basis of the exceptional stretchability of elastomer substrates rather than the stretchability of the materials themselves.[26,27] It is speculated that the extreme stretchability of our composite material is attributable mainly to the inter- and intra-morphology of 3D-Cs. The basic morphology of elastomeric, thermoplastic triblock copolymers is based on the separated compartment of a soft part with a low glass transition temperature (T_g) and a rigid part with a much higher T_g.[28] This indicates that when conductive moieties are incorporated into the elastomer matrix, it would be better to occupy it separately with continuous spatial distribution to endow both conductivity and stretchability. As shown in Figure S8 (Supporting Information), the 3D-C/MWCNT framework material fits such macroscopic morphological requisites, as the individual 3D-C was connected by the network of MWCNTs, leaving behind a spatial void where the elastomeric polymer can be taken between neighboring 3D-Cs. The elastomer region containing the majority of the fillers in the composites behaves as the rigid part of the elastomer itself, and the filler-free elastomer region still preserves its elastic property (Figure 4b). Furthermore, the intramorphology consisting of flexible, slightly stretchable carbon sheets allows for the structural expandability in elastomeric matrix, as proposed in previously reported structure-engineered CNT forests.[16] In only CNT-incorporated stretchable conductors, the conductivity can be varied significantly depending on stretching conditions, as the spatial orientation of CNTs is determined by the external forces, giving the critical impact to electrical properties of films.[29] In composite systems, the CNT acts as a one-dimensional conducting pathway with a low volumetric threshold for percolation conduction, and the electrical conductivity in overall film is determined by additionally incorporated conducting constituent materials;[11,14] in this case, the CNTs are adhered firmly to other constituent materials, and the CNTs are not oriented freely depending on the

DOI: 10.1021/am5080634
ACS Appl. Mater. Interfaces 2015, 7, 4109−4117

external forces. As seen in Figure S9 (Supporting Information), in our study, the spatial arrangement of CNTs were not varied during stretching under a strain of 50%. It is believed that this is another evidence for the fact that the electrical conductivity was not changed significantly for our MWCNT/3D-C composite electrodes even under harsh stretching conditions. In order to improve further the electrical conductivity, the additional incorporation of highly conductive metallic moieties has been underway into well-designed stretchable composites. It is highly expected that more conductive, stretchable composite materials are achievable with the incorporation of metallic nanoparticles, which can undergo the morphological densification at low temperatures, or one-dimensional metallic nanowires with a low volumetric threshold for percolation-based electrical conduction.

Figure 4c and Video S1 (Supporting Information) show the variation of normalized resistance during a repeated stretching test under a strain of 50%. In wearable electronics, where stretchable conductors would be widely adopted as initial, principal applications, the strain range of 30−50% is high enough to be applicable to the knee or elbow of the human body. To obtain accurate information on repeated stretching properties, we formed Al foil electrodes in regions held by a side-end zig of a stretching machine; when the resistance was measured while the probes of the ohm-meter were attached in the middle of the films, the part of the film between two probes was not entirely stretched, with an improper result showing no variation of normalized resistance for prolonged repeated stretching tests. It is clearly observed that the resistance was not altered even during 1000 cycles, except for the initial increase of resistance, commonly observed in polymer-based stretchable conductors.[30] Such mechanical stability against external applied force for deforming the film structure was also confirmed by the fact that, even under a folding test with a bending radius of 450 μm, the film conductivity was not varied at all (Figure 4d).

The direct-printability of the stretchable conducting pastes was tested using a programmable dispenser without the need of prepatterned masks. To date, the exploitation of stretchable conducting pastes has been based on monitoring both the electrical and stretching properties of resulting films without the demonstration of direct-printability, except for the limited number of studies.[8,14,31] In stretchable electronics, programmable-dispensing techniques are advantageous over other printing methods, including gravure(-offset) printing, reverse-offset printing, inkjet printing, and screen printing, because it is a noncontact printing method with no necessity of a prepatterned mask/mold and rheologically appropriateness for viscous fluids incorporating a high amount of polymer. In particular, the noncontact, direct-writing capability is of paramount importance in generating on-demand patterned structures on elastomeric substrates with low elastic moduli. The 3D-C/MWCNT/SIS paste prepared in this study showed the rheological properties, with a storage modulus of 2.1 KPa and a complex viscosity of 330 Pa·s, adequate for a dispensing printing technique (Figure S10, Supporting Information). As shown in Figure 5, the printed composite electrode was still active as a conductor after being printed in a curved geometry, even with an angle of 105°. In this study, the pattern resolution was limited due to the use of a nozzle with an inner diameter of 350 μm. Narrowing the pattern line width is currently underway by the use of a nozzle with a smaller inner diameter and application of voltage around the nozzle to producing a more concentrated jet-flow, as demonstrated in electrohydrodynamic-jet printing.[32,33] As a further study, the additional incorporation of metallic conducting fillers in the form of nanowires, nanoparticles, or flakes would be investigated with sophisticatedly designed material layouts in composites for preserving the intra- and interconductive pathways.

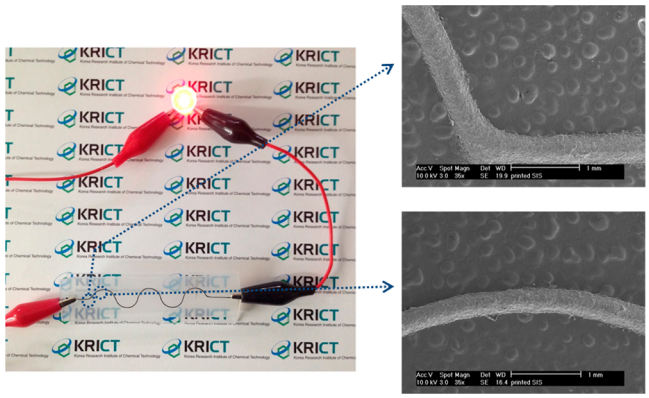

Figure 5. Photograph and SEM images for directly printed MWCNT/3D-C composite electrodes. The weight ratio of MWCNT to 3D-C was 3:3.

4. CONCLUSIONS

We have demonstrated that hierarchically structured RGO-Ni-graphene composite materials successfully allow for the formation of highly stable, stretchable conductors showing improved mechanical and electrical properties in comparison with previously reported carbon-based counterparts. Three-dimensionally stacked composite materials with a characteristic intrastructure were synthesized through an easily scalable mixing process between graphene oxides and Ni nanoparticles, followed by annealing at an elevated temperature and a CVD-graphene growth process. The free-standing films derived from the mixture of the resulting composite material and SIS elastomeric polymer exhibited stretchability up to 300%, without the use of prestrained substrates, and the normalized conductivity variation of only 0.34 under a strain of 300%. In addition, the morphological and electrical stability, under an extreme folding condition with a bending radius of 450 μm, was evaluated with a measurement of unchanged resistance. The direct-patternability using a mask-free, programmable disperser was demonstrated with the generation of active electrodes even in printed geometries. It is believed that the newly developed methodology of preparing carbon-based composite materials for application as stretchable conductors could pave the way to exploiting the new design concept beyond the limits of precedent carbon-based stretchable conductors.

■ ASSOCIATED CONTENT

Supporting Information

Experimental details, SEM image, HRTEM image, XPS Ni 2p spectrum, XRD results, and TGA results for synthesized Ni nanoparticles, the conductivity variations for MWCNT/GO and MWCNT/cRGO conductors, SEM image for MWCNT/3D-C composite material, rheological properties of prepared MWCNT/3D-C paste, and video file for 1000 times repeated stretching test. This material is available free of charge via the Internet at http://pubs.acs.org.

DOI: 10.1021/am5080634
ACS Appl. Mater. Interfaces 2015, 7, 4109−4117

AUTHOR INFORMATION

Corresponding Authors

*E-mail: sunsukl@krict.re.kr.

*E-mail: sjeong@krict.re.kr.

Notes

The authors declare no competing financial interest.

ACKNOWLEDGMENTS

This research has been supported by the Korea Research Institute of Chemical Technology (KRICT) core project (KK-1402-C0) funded by the Ministry of Science, ICT and Future Planning. This work is also partially supported by a grant (2011-0031636) from the center for Advanced Soft Electronics under the Global Frontier Research Program of the Ministry of Science, ICT and Future Planning.

REFERENCES

(1) Park, M.; Park, J.; Jeong, U. Design of Conductive Composite Elastomers for Stretchable Electronics. *Nano Today* **2014**, *9*, 244−260.

(2) Yang, C.; Wong, C. P.; Yuen, M. M. F. Printed Electrically Conductive Composites: Conductive Filler Designs and Surface Engineering. *J. Mater. Chem. C* **2013**, *1*, 4052−4069.

(3) Deng, H.; Lin, L.; Ji, M.; Zhang, S.; Yang, M.; Fu, Q. Progress on the Morphological Control of Conductive Network in Conductive Polymer Composites and the Use as Electroactive Multifunctional Materials. *Prog. Polym. Sci.* **2014**, *39*, 627−655.

(4) Park, M.; Im, J.; Shin, M.; Min, Y.; Park, J.; Cho, H.; Park, S.; Shim, M. B.; Jeon, S.; Chung, D. Y.; Bae, J.; Park, J.; Jeong, U.; Kim, K. Highly Stretchable Electric Circuits from a Composite Material of Silver Nanoparticles and Elastomeric Fibers. *Nat. Nanotechnol.* **2012**, *7*, 803−809.

(5) Yamada, T.; Hayamizu, Y.; Yamamoto, Y.; Yomogida, Y.; Izadi-Najafabadi, A.; Futaba, D. N.; Hata, K. A Stretchable Carbon Nanotube Strain Sensor for Human-Motion Detection. *Nat. Nanotechol.* **2011**, *6*, 296−301.

(6) Yu, B.; Zhou, F.; Liu, G.; Liang, Y.; Huck, W. T.; Liu, W. The Electrolyte Switchable Solubility of Multi-Walled Carbon Nanotube/Ionic Liquid (MWCNT/IL) Hybrids. *Chem. Commun.* **2006**, 2356−2358.

(7) Sekitani, T.; Noguchi, Y.; Hata, K.; Fukushima, T.; Aida, T.; Someya, T. A Rubberlike Stretchable Active Matrix Using Elastic Conductors. *Science* **2008**, *321*, 1468−1472.

(8) Sekitani, T.; Nakajima, H.; Maeda, H.; Fukushima, T.; Aida, T.; Hata, K.; Someya, T. Stretchable Active-Matrix Organic Light-Emitting Diode Display Using Printable Elastic Conductors. *Nat. Mater.* **2009**, *8*, 494−499.

(9) Kim, T. A.; Kim, H. S.; Lee, S. S.; Park, M. Single-Walled Carbon Nanotube/Silicone Rubber Composites for Compliant Electrodes. *Carbon* **2012**, *50*, 444−449.

(10) Shang, S.; Zeng, W.; Tao, X.-M. High Stretchable MWNTs/Polyurethane Conductive Nanocomposites. *J. Mater. Chem.* **2011**, *21*, 7274−7280.

(11) Chun, K.-Y.; Oh, Y.; Rho, J.; Ahn, J.-H.; Kim, Y.-J.; Choi, H. R.; Baik, S. Highly Conductive, Printable and Stretchable Composite Films of Carbon Nanotubes and Silver. *Nat. Nanotechnol.* **2010**, *5*, 853−857.

(12) Ma, R.; Lee, J.; Choi, D.; Moon, H.; Baik, S. Knitted Fabrics Made from Highly Conductive Stretchable Fibers. *Nano Lett.* **2014**, *14*, 1944−1951.

(13) Ma, R.; Kwon, S.; Zheng, Q.; Kwon, H. Y.; Kim, J. I.; Choi, H. R.; Baik, S. Carbon-Nanotube/Silver Networks in Nitrile Butadiene Rubber for Highly Conductive Flexible Adhesives. *Adv. Mater.* **2012**, *24*, 3344−3349.

(14) Chun, K.-Y.; Kim, S. H.; Shin, M. K.; Kim, Y. T.; Spinks, G. M.; Aliev, A. E.; Baughman, R. H.; Kim, S. J. Free-Standing Nanocomposites with High Conductivity and Extensibility. *Nanotechnology* **2013**, *24*, 165401−165410.

(15) Li, Y.; Shimizu, H. Toward a Stretchable, Elastic, and Electrically Conductive Nanocomposite: Morphology and Properties of Poly[styrene-*b*-(ethylene-co-butylene)-*b*-styrene]/Multiwalled Carbon Nanotube Composites Fabricated by High-Shear Processing. *Macromolecules* **2009**, *42*, 2587−2593.

(16) Shin, M. K.; Oh, J.; Lima, M.; Kozlov, M. E.; Kim, S. J.; Baughman, R. H. Elastomeric Conductive Composites Based on Carbon Nanotube Forests. *Adv. Mater.* **2010**, *22*, 2663−2667.

(17) Luo, B.; Zhi, L. Design and Construction of Three Dimensional Graphene-Based Composites for Lithium Ion Battery Applications. *Energy Environ. Sci.* **2015**, *8*, 456−477.

(18) Sudeep, P. M.; Narayanan, T. N.; Ganesan, A.; Shaijumon, M. M.; Yang, H.; Ozden, S.; Patra, P. K.; Pasquali, M.; Vajtai, R.; Ganguli, S.; Roy, A. K.; Anantharaman, M. R.; Ajayan, P. M. Covalently Interconnected Three-Dimensional Graphene Oxide Solids. *ACS Nano* **2013**, *7*, 7034−7040.

(19) Yan, Z.; Ma, L.; Zhu, Y.; Lahiri, I.; Hahm, M. G.; Liu, Z.; Yang, S.; Xiang, C.; Lu, W.; Peng, Z.; Sun, Z.; Kittrell, C.; Lou, J.; Choi, W.; Ajayan, P. M.; Tour, J. M. Three-Dimensional Metal−Graphene−Nanotube Multifunctional Hybrid Materials. *ACS Nano* **2013**, *7*, 58−64.

(20) Jeong, S.; Lee, S. H.; Jo, Y.; Lee, S. S.; Seo, Y.-H.; Ahn, B. W.; Kim, G.; Jang, G.-E.; Park, J.-U.; Ryu, B.-H.; Choi, Y. Air-Stable, Surface-Oxide Free Cu Nanoparticles for Highly Conductive Cu Ink and Their Application to Printed Graphene Transistors. *J. Mater. Chem. C* **2013**, *1*, 2704−2710.

(21) Oh, S.-J.; Jo, Y.; Lee, E. J.; Lee, S. S.; Kang, Y. H.; Jeon, H.-J.; Cho, S. Y.; Park, J.-S.; Seo, Y.-H.; Ryu, B.-H.; Choi, Y.; Jeong, S. Ambient Atmosphere-Processable, Printable Cu Electrodes for Flexible Device Applications: Structural Welding in a Milisecond Timescale of Surface Oxide-Free Cu Nanoparticles. *Nanoscale*, DOI: 10.1039/C4NR06816E.

(22) Jeong, S.; Song, H. C.; Lee, W. W.; Lee, S. S.; Choi, Y.; Son, W.; Kim, E. D.; Paik, C. H.; Oh, S. H.; Ryu, B.-H. Stable Aqueous Based Cu Nanoparticle Ink for Printing Well-Defined Highly Conductive Features on a Plastic Substrate. *Langmuir* **2011**, *27*, 3144−3149.

(23) Jo, Y.; Oh, S.-J.; Lee, S. S.; Seo, Y.-H.; Ryu, B.-H.; Choi, Y.; Jeong, S. Highly Flexible, Rollable, Printable Ag Conductive Features on PET and Paper Substrates via Instant Continuous Photonic Sintering in a Large Area. *J. Mater. Chem. C* **2014**, *2*, 9746−9753.

(24) Jeong, S.; Woo, K.; Kim, D.; Lim, S.; Kim, J. S.; Shin, H.; Xia, Y.; Moon, J. Controlling the Thickness of the Surface Oxide Layer on Cu Nanoparticles for the Fabrication of Conductive Structures by Ink-Jet Printing. *Adv. Funct. Mater.* **2008**, *18*, 679−686.

(25) Fukushima, T.; Aida, T. Ionic Liquids for Soft Functional Materials with Carbon Nanotubes. *Chem.—Eur. J.* **2007**, *13*, 5048−5058.

(26) Won, Y.; Kim, A.; Yang, W.; Jeong, S.; Moon, J. A Highly Stretchable, Helical Copper Nanowire Conductor Exhibiting a Stretchability of 700%. *NPG Asia Mater.* **2014**, *6*, e132.

(27) Lee, P.; Lee, J.; Lee, H.; Yeo, J.; Hong, S.; Nam, K. H.; Lee, D.; Lee, S. S.; Ko, S. H. Highly Stretchable and Highly Conductive Metal Electrode by Very Long Metal Nanowire Percolation Network. *Adv. Mater.* **2012**, *24*, 3326−3332.

(28) Young, R. J.; Lovell, P. A. *Introduction to Polymers*; Chapman & Hall: London, 1994; pp 304−305.

(29) Lin, L.; Liu, S.; Fu, S.; Zhang, S.; Deng, H.; Fu, Q. Fabrication of Highly Stretchable Conductors via Morphological Control of Carbon Nanotube Network. *Small* **2013**, *9*, 6320−3629.

(30) Kim, T.; Song, H.; Kim, S.; Kim, D.; Chung, S.; Lee, J.; Hong, Y. Inkjet-Printed Stretchable Single-Walled Carbon Nanotube Electrodes with Excellent Mechanical Properties. *Appl. Phys. Lett.* **2014**, *104*, 113103.

(31) Kim, S.; Byun, J.; Choi, S.; Kim, D.; Kim, T.; Chung, S.; Hong, Y. Negatively Strain-Dependent Electrical Resistance of Magnetically Arranged Nickel Composites: Application to Highly Stretchable Electrodes and Stretchable Lighting Devices. *Adv. Mater.* **2014**, *26*, 3094.

DOI: 10.1021/am5080634
ACS Appl. Mater. Interfaces 2015, 7, 4109−4117

(32) Jeong, S.; Lee, J.-Y.; Lee, S. S.; Seo, Y.-H.; Kim, S.-Y.; Park, J.-U.; Ryu, B.-H.; Yang, W.; Moon, J.; Choi, Y. Metal Salt-Derived In−Ga−Zn−O Semiconductors Incorporating Formamide as a Novel Co-solvent for Producing Solution-Processed, Electrohydrodynamic-Jet Printed, High-Performance Oxide Transistors. *J. Mater. Chem. C* **2013**, *1*, 4236−4243.
(33) Park, J.-U.; Hardy, M.; Kang, S. J.; Barton, K.; Adair, K.; Mukhopadhyay, D. K.; Lee, C. Y.; Strano, M. S.; Alleyne, A. G.; Georgiadis, J. G.; Ferreira, P. M.; Rogers, J. A. High-Resolution Electrohydrodynamic Jet Printing. *Nat. Mater.* **2007**, *6*, 782−789.

DOI: 10.1021/am5080634
ACS Appl. Mater. Interfaces 2015, 7, 4109−4117